

An X-Ray Penumbra Imager for Measurements of Electron-Temperature Profiles in Inertial Confinement Fusion Implosions on OMEGA

P. J. Adrian,¹ J. A. Frenje,¹ B. Aguirre,² B. Bachmann,³ A. Birkel,¹ M. Gatu Johnson,¹ N. V. Kabadi,¹ B. Lahmann,¹ C. K. Li,¹ O. M. Mannion,⁴ W. Martin,² Z. L. Mohamed,⁴ S. P. Regan,⁴ H. G. Rinderknecht,⁴ B. Scheiner,⁵ M. J. Schmitt,⁵ F. H. Séguin,¹ R. C. Shah,⁴ H. Sio,³ C. Sorce,⁴ G. D. Sutcliffe,¹ and R. D. Petrasso¹

¹Plasma Science and Fusion Center, Massachusetts Institute of Technology

²Sandia National Laboratories

³Lawrence Livermore National Laboratory

⁴Laboratory for Laser Energetics, University of Rochester

⁵Los Alamos National Laboratory

One of the main challenges of inertial confinement fusion is symmetry control of the implosion. Asymmetries reduce implosion performance and generate bulk flows that degrade the conversion of shell kinetic energy into hot-spot thermal energy. Recently, penumbral imaging of hot-spot x-ray emission was used at the National Ignition Facility to simultaneously measure hot-spot shape and temperature to assess asymmetry in different implosion designs,¹ as well as spatially resolve electron temperature to quantify mix-induced radiative cooling.² Penumbral imaging is a coded imaging technique, where a source of size S is imaged with an aperture of radius R_{app} such that $2R_{\text{app}} > S$. This imaging technique is used when signal statistics prevent the use of conventional pinhole imaging ($2R_{\text{app}} \ll S$). Information about spatial distribution of the emitting source is encoded in the penumbra.

We developed and fielded a new penumbral imager at the Omega Laser Facility, with 6- μm resolution, to image x rays in the energy range of 10 to 30 keV. This system is based on the existing penumbral charged-particle imaging system (PCIS).³ Three imagers can be fielded in different ten-inch diagnostic manipulators (TIM's) to study 3-D asymmetries. We record images in different x-ray energy bands using a filtered stack of FujiTM image plates and present a technique to infer the radially dependent electron temperature $T_e(r)$.

The PCIS detectors are TIM-based diagnostics that hold an aperture 4.2 cm from the target chamber center and a detector 59 cm from the aperture, yielding a magnification of ~ 14 . Three types of apertures are used: $1 \times 2000 \mu\text{m}$, $19 \times 400 \mu\text{m}$, or $151 \times 100 \mu\text{m}$ (number of pinholes \times diameter) made from a substrate of 500- μm -thick Ta, 125- μm -thick W, or 125- μm -thick W, respectively. All apertures are circular to less than 3 μm . The detector is an array of FujiTM SR x-ray image plates interspersed with x-ray filters. Each subsequent image plate is sensitive to a higher-energy portion of the x-ray spectrum: typical values for peak sensitivity range from 10- to 30-keV x rays. The image plates are scanned with 25- μm resolution. The spatial resolution of the system at a magnification of 14 is 6 μm and is limited by the combination of detector resolution and x-ray diffraction.

A burn-averaged T_e is extracted from the inferred x-ray spectrum, which is derived from the energy deposited in each penumbral image. The image-plate scanner measures the photostimulated luminescence (PSL), which is related to the energy deposited in the phosphor layer. The PSL recorded in the umbra of the k th image plate is calculated as

$$\text{PSL}_k = \int_0^\infty \frac{\text{IP}_{\text{sen}}(E)}{F_k(t)} \frac{j(E)}{E} T_k(E) dE, \quad (1)$$

where E is the x-ray energy, $IP_{\text{sen}}(E)$ is the image-plate sensitivity in PSL/photon, $F_k(t)$ represents the fading of the image plate when it is scanned t minutes after exposure, $j(E)/E$ is the photon emission in photons/keV, and $T_k(E)$ is the transmission function of all filters in front of the k th image plate. The spectrum is modeled as a single-temperature bremsstrahlung emission $j(E) = A \exp(-E/T_e)$, where A and T_e are the fit variables. The main sources of error in this analysis were due to photon statistics and uncertainty in the fade curve of each image plate.

The source profile is reconstructed from the measured penumbral image using an iterative deconvolution approach based on the Lucy–Richardson algorithm.⁴ On each iteration the source image is convolved with the aperture function and compared against the measured penumbral image using a χ^2 metric. Iterations stop once the reduced χ^2 metric is of the order of unity or lower. For x-ray penumbral imaging, we have found that signal statistics are excellent for x rays in the energy range of 10 to 30 keV for most implosions of interest.

Figure 1 shows [(a),(b)] penumbral images and [(c),(d)] reconstructions from a SiO_2 capsule with 422- μm radius, 2.4- μm shell thickness, gas fill of 10 atm D_2 , 15 atm ^3He , and ~ 0.04 atm T_2 , and imploded with 15.6 kJ of laser energy in a 0.6-ns square pulse. Both reconstructions converged in 100 iterations and show a ring-like structure resulting from the unablated glass shell that surrounds the hot spot.

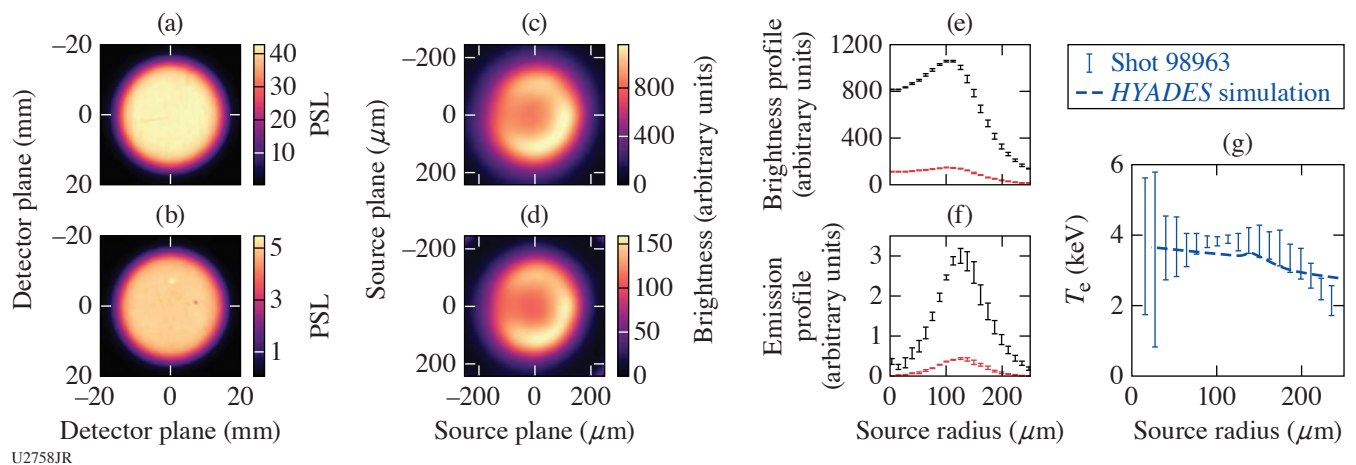


Figure 1
Data from shot 98963. The x-ray penumbral imager used a 1000- μm -radius aperture. (a) Recorded x-ray penumbral image closest to target chamber center (TCC) with 15 μm Ta + 3000 μm CR-39 ($\text{C}_{12}\text{H}_{18}\text{O}_7$) + 100- μm Al filtering. (b) X-ray penumbral image for the image plate farthest from TCC with additional 150- μm Al filtering [(c),(d)]. Reconstructed x-ray emission obtained from (a) and (b), respectively. (e) Azimuthally averaged brightness profiles (chord integrated) from (c) and (d) in black and red, respectively. (f) Radial emission profiles calculated from the surface brightness profiles in (e) via Abel inversion. (g) Measured $T_e(r)$ for shot 98963 (blue error bars). A post-shot *HYADES* simulation is shown (dashed blue line). The simulated T_e is an x-ray emission averaged over the entire implosion time.

From these measurements, the radial profile of T_e is determined. We assume spherical symmetry of the source, which allows us to azimuthally average the reconstructed x-ray images to get the brightness profile shown in Fig. 1(e). The errors in the brightness profiles are determined from the azimuthal variation in each radial bin. To extract $T_e(r)$, we calculate the radial emission from the brightness profiles by an inverse Abel transform [Fig. 1(f)]. We use a discrete version of the Abel transform proposed by Yoshikawa and Suto.⁵

The relative amplitude of the radial emission profiles is used to infer T_e in each radial bin by using Eq. (1) and filtering of the two images. A post-shot simulation of this implosion was performed using the *HYADES* 1-D radiation-hydrodynamics code,⁶ and the emission-averaged $T_e(r)$ is shown in Fig. 1(g) for comparison. The measured $T_e(r)$ agrees with the simulation. The average uncertainty in $T_e(r)$ is 10%. The best inference of the temperature is where the most x-ray emission occurs. However, there are

large uncertainties at small radii due to low levels of emission occurring at those small radii. In the future, this technique will be extended to utilize three simultaneous lines of sight to reconstruct 3-D maps of electron temperature.

This material is based upon work supported by the Department of Energy National Nuclear Security Administration under Award Number DE-NA0003856, the University of Rochester, and the New York State Energy Research and Development Authority.

1. B. Bachmann *et al.*, Rev. Sci. Instrum. **87**, 11E201 (2016).
2. B. Bachmann *et al.*, Phys. Rev. E **101**, 033205 (2020).
3. F. H. Séguin *et al.*, Rev. Sci. Instrum. **75**, 3520 (2004).
4. W. H. Richardson, J. Opt. Soc. Am. **62**, 55 (1972).
5. K. Yoshikawa and Y. Suto, Astrophys. J. **513**, 549 (1999).
6. J. T. Larsen and S. M. Lane, J. Quant. Spectrosc. Radiat. Transf. **51**, 179 (1994).